3D VSP imaging under a complex salt finger at Atlantis, Gulf of Mexico

Chang-Chun Lee, Jing Yang, CGG*

Robert Chrisman, Jean-Paul Van Gestel, Mark Benson, BP

Summary

To improve image resolution in the vicinity of the well, 3D vertical seismic profile (VSP) data was acquired at the Atlantis field in the Gulf of Mexico (GoM) to complement the existing towed-streamer and ocean-bottom node (OBN) data. Two unique data challenges require special consideration and innovative techniques in order to unlock the full imaging potential at the Atlantis field: (1) illumination issues related to the receivers being placed in a well that goes through a complicated salt finger; (2) receiver reorientation issues related to the survey's two-phase acquisition due to receivers being pulled out and placed back into the well. We demonstrate how we mitigate the impact of these challenges through improved XYZ vector fidelity reorientation and least-squares reverse time migration (LSRTM).

Introduction

The Atlantis field, one of the giant fields in the Gulf of Mexico (GoM), was discovered in 1998 and began producing in 2007. The field is located in Green Canyon, 130 miles from the coast of Louisiana. Like many subsalt fields in the GoM, seismic imaging at Atlantis is very challenging due to complex salt structures in the overburden (Figure 1). Recently, great efforts were made to obtain a better tilted transverse isotropic (TTI) velocity model for the Atlantis field using multi-wide azimuth and ocean-bottom node (OBN) data (Roberts et al., 2011; Shen et al., 2017). Yet 3D vertical seismic profile (VSP) surveys may offer even better opportunities to obtain high-quality images near the wellbore compared to surface steamer and OBN data due to the fact that the wave propagation is less distorted by salt since the receivers are generally placed below the salt. To assist the continued development of the Atlantis field in the GoM, 3D VSP data was acquired in October 2017, intending to complement the existing towed-streamer and OBN data. The Atlantis VSP survey featured a shot coverage of approximately 10 x 16 km at the surface with 100 receivers placed down the well at a 65.6-foot interval, down to 16,600 ft. Each receiver consisted of three individual geophones, i.e., XYZ components, mounted orthogonally to each other.

Two unique challenges make the Atlantis VSP survey different from other VSP surveys and need special accommodations in the processing and imaging workflow. The first challenge is related to the area's complex geology. In order to obtain high-quality images right below the complex salt finger structure, 100 receivers were placed into the well, going through the complicated salt finger. As a result, strong amplitude variation across the receivers was observed. Due to the presence of salt around the shallow receivers, direct arrival energy mixed with refraction energy even at near offsets. The complexity caused by the salt was challenging for XYZ vector fidelity reorientation and resulted in strong illumination variation in the migrated receiver gathers. The second challenge is related to the unique acquisition of the Atlantis VSP survey. During acquisition, the receivers had to be pulled out of the wellbore due to Hurricane Nate. After placing the receivers back into similar positions in the wellbore, the second phase of shots was completed. As a result, two sets of reorientation angles were needed to calibrate the orientation of each receiver for the phase I and phase II data (inset in Figure 1). To obtain a reliable VSP image, these unique challenges must be addressed, especially for XYZ vector fidelity reorientation.

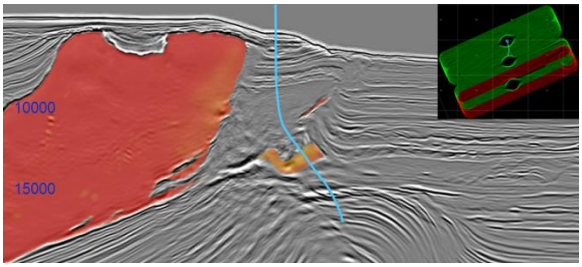

Figure 1: A section view showing the challenges of the Atlantis field due to complex salt geometry (intidated by red and orange (dirty salt) color). Well trajectory is indicated by the blue line. The inset shows the shot locations for phase I (red) and phase II (green) shots.

XYZ vector fidelity reorientation

After placing the receivers downhole, the orientation of each is unknown; thus, aligning all the receivers to the same orientation (Cardinal directions and true vertical) is critical.

To ensure constructive stacking among all the downhole receivers, calibration of the orientation of each receiver is necessary. Similar to the approach applied on earlier VSP data, we applied an algorithm using 3D TTI elastic modeled synthetic data to calibrate the orientation for each receiver (Dy et al., 2016). This amplitude-based algorithm minimizes the objective function of $|\vec{\boldsymbol{A}} - \vec{\boldsymbol{R}}^{-1}\vec{\boldsymbol{A}'}|$ by scanning all possible rotations to find $\vec{\boldsymbol{R}}$, where $\vec{\boldsymbol{A}}$ is the 3C field data from the real data, $\vec{\boldsymbol{A}'}$ is the 3C field data from the modeled data, and $\vec{\boldsymbol{R}}$ is the unknown tilt correction

10.1190/segam2018-2996268.1

matrix. To achieve a reasonable result for XYZ vector fidelity reorientation, direct arrivals on both the modeled data and real data need to be accurately picked to obtain amplitude information.

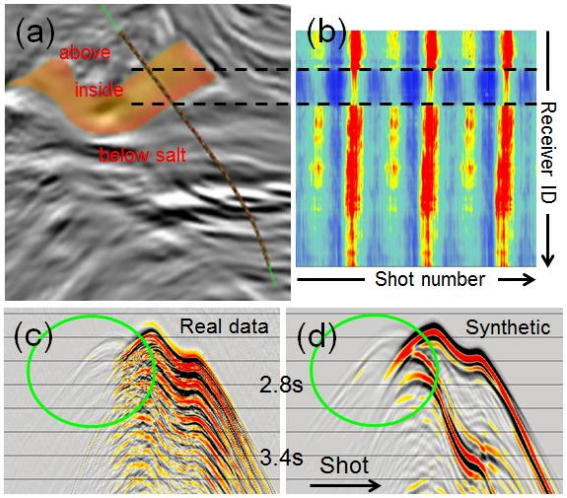

Figure 2: (a) A section view showing the complicated salt finger geology around the receivers. The dark brown color indicates receiver locations. (b) An amplitude slice from 2-8 s of data showing the amplitude variation across receivers due to the complicated salt geometry. (c) and (d) Receiver gathers from real and modeled synthetic data, respectively, showing refraction energy can mix with direct arrival energy on near offset data.

One of the difficulties in XYZ vector fidelity reorientation for Atlantis VSP is related to the receiver locations passing through the complicated salt finger. For shallow receivers located inside and around the salt finger area, the direct arrival amplitudes are weak and mixed with salt-related refraction energy, even in the near and middle offsets (Figure 2). This results in inaccurate direct arrival picking, which will cause incorrect rotation angle calculations using the amplitude-based algorithm. To overcome this issue, an alternative crosscorrelation-based algorithm was developed. The objective function for the crosscorrelation-based algorithm was changed to $\left|\left(\overrightarrow{\boldsymbol{A_X}} * \overrightarrow{\boldsymbol{A_Z}} - \vec{\boldsymbol{R}}^{-1}\overrightarrow{\boldsymbol{A'_X}} * \vec{\boldsymbol{R}}^{-1}\overrightarrow{\boldsymbol{A'_Z}}\right)^2 + \left(\overrightarrow{\boldsymbol{A_Y}} * \overrightarrow{\boldsymbol{A_Z}} - \vec{\boldsymbol{R}}^{-1}\overrightarrow{\boldsymbol{A'_Y}} * \vec{\boldsymbol{R}}^{-1}\overrightarrow{\boldsymbol{A'_Z}}\right)^2\right|$, where $*$ represents the crosscorrelation operator. The advantage of using the crosscorrelation algorithm is that it is less sensitive to inaccurate direct arrival picking. Moreover, angle constraints for X (related to well azimuth angle) and Z (related to well tilt angle) were used to further restrict the possible rotation angles because of the physical angle limit for the receivers inside the casing. Figure 3 shows the reorientation result comparison using the amplitude-based algorithm (Figure 3b) and the crosscorrelation-based algorithm with angle constraints (Figure 3c). We can see that the crosscorrelation algorithm with angle constraints provided more coherent energy in shot gathers for shallow receivers after reorientation, and the obtained X and Z angles followed the well deviation angles.

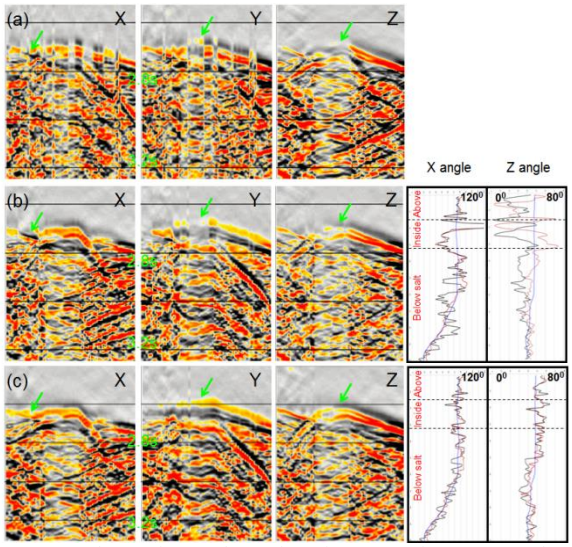

Figure 3: The receiver gathers of receivers 1-50 for X-, Y-, and Z-components (a) before reorientation, (b) after reorientation with the amplitude-based algorithm, and (c) after reorientation with the crosscorrelation-based algorithm with X and Z angle constraints. The plots on the right (x-axis:angle, y-axis:receiver number) show the obtained reorientation X and Z angles for phase I (black) and phase II (red) data compared to the well deviation X and Z angles (blue). The results from (c) show more coherent energy in the shot gathers, and the angle plots follow the well deviation angles.

The second difficulty of XYZ vector fidelity reorientation is related to the Atlantis VSP acquisition, where two sets of rotation angles are required to calibrate the orientation of the receivers before and after they were pulled out from wellbore. Phase I data does not include near offset data, which significantly degraded the direct arrival picking quality, especially for shallow receivers. To overcome the lack of near offset data for phase I, an anchor method was used for XYZ vector fidelity reorientation of the shallow receivers from the phase I data. During the acquisition, one sequence (source line) was reshot in phase II at the shot locations of phase I. The common shots for phase I data and phase II data were used for the anchor method. Instead of using modeled data, the phase I data was anchored to the rotated real data from phase II to find the rotation angles for the shallow receivers using the shots common to both phases. Figure 4 shows the reorientation result with and without the anchor method. We can see that the energy around the shallow receivers became more coherent with the anchor method. The crosscorrelation (between Y and Z components) map consisting of all the shots from both phases I and II also shows consistent amplitude between

10.1190/segam2018-2996268.1

the boundary of phase I and II with the anchor method (Figure 4f), and is comparable to the map from synthetic data (Figure 4c).

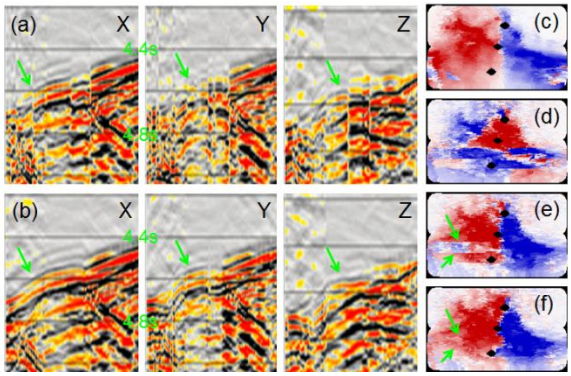

Figure 4: The impact of the anchor method on the reorientation result. Receiver gathers of receivers 1-50 for X-, Y-, and Z-components after reorientation (a) without anchor method and (b) with anchor method. Y/Z component crosscorrelation map QC for (c) synthetic data, (d) real data before reorientation, (e) real data after reorientation without the anchor method, and (f) real data after reorientation with the anchor method, where the crosscorrelation map shows consistent value across phase I and II data and is comparable to the map from synthetic data.

With the benefits and improvements from the crosscorrelation algorithm, X and Z angle constraints, and the anchor method for phase I shallow receivers, the impact of the XYZ vector fidelity reorientation on the migrated stacked images is shown in Figure 5b. We see significant improvement in the migrated images after XYZ vector fidelity reorientation for X- and Y-components due to the constructive stacking among all the receivers. This will also lead to a more coherent and higher resolution image after merging of XYZ components.

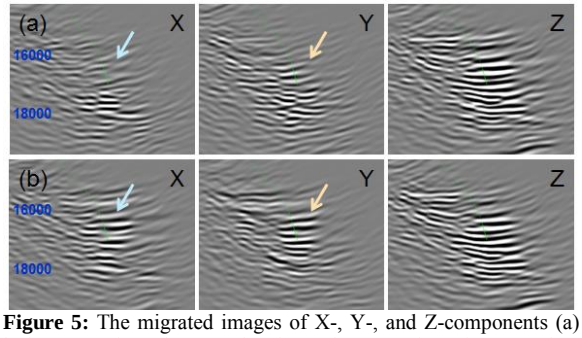

Figure 5: The migrated images of X-, Y-, and Z-components (a) before reorientation and (b) after reorientation. Before reorientation, the stacked images for all receivers of X and Y components are relative poor due to the random orientation for the X and Y components. After reorientation, the energy can be stacked constructively among receivers and the image shows stronger and more coherent events.

VSP Least-squares RTM

In the Atlantis VSP survey, receivers were placed above, inside, and below the salt finger. Strong amplitude variation is observed across the receivers (Figure 2b), and a strong illumination pattern is observed on the migrated receiver gathers. In order to compensate for the amplitude variation across receivers, least-squares RTM (LSRTM) (Wang et al., 2016) was performed receiver-by-receiver. The data for each receiver was de-migrated and re-migrated separately, and a curvelet Hessian filter was designed by matching individual receiver images to a reference reflectivity in the curvelet domain. The Hessian filter was then applied to individual receiver data to compensate for illumination loss and acquisition footprint. Besides compensating for the illumination loss, another benefit to the image is a reduction in swing noise caused by migration, which is usually quite severe in the VSP migrated image. Figure 6 shows the impact of LSRTM on the migrated receiver gathers and stacked image. We can see that LSRTM balanced the amplitude of the image and increased its interpretability. The strong illumination variation observed on the receiver gathers was also greatly reduced after LSRTM, and the amplitude was more consistent across the receivers. From the receiver gathers after LSRTM, we can also observe that the receivers inside the salt finger still significantly contribute to the image, while the receivers above the salt finger contribute much less.

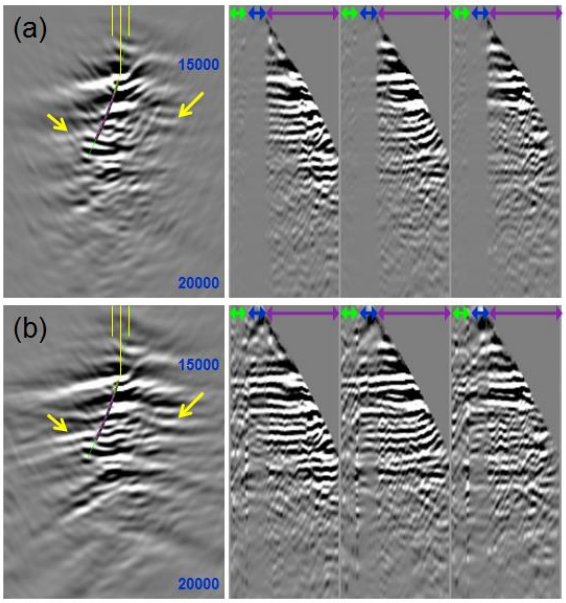

Figure 6: The impact of LSRTM: (a) before and (b) after LSRTM for 3D VSP data. The left side shows the migrated stacked image and right side shows the receiver gathers (receivers above salt: green arrow; inside salt: blue arrow; below salt: purple arrow).

10.1190/segam2018-2996268.1

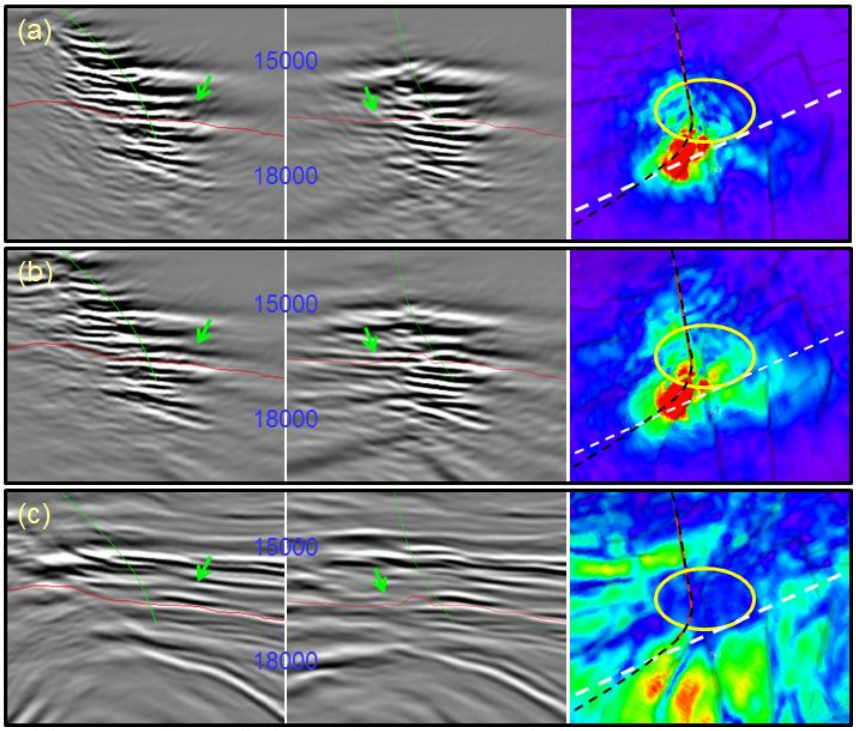

Figure 7: RTM images and the corresponding amplitude extraction maps on a target horizon (a) before LSRTM, (b) after LSRTM, and (c) legacy streamer and OBN image. Left panel shows the seismic image along well trajectory (black-dashed line on the map), and middle panel shows the seismic image along cross-line direction (white-dashed line on the map). After LSRTM, the illuminated area gets expanded, and the swing noise gets reduced. The area that cannot be imaged by streamer and OBN data can now be imaged by VSP data.

Figure 7 shows that after LSRTM, the illuminated area gets expanded by enhancing the event signals while not boosting the swing noise (Figure 7b). From the amplitude extraction map, we can see the weak illumination zone beneath receivers from the streamer and OBN data due to the complicated overburden (Figure 7c, yellow circle on the right panel). For receivers below the salt finger, wave propagation of the VSP data is less distorted. Hence, the VSP images provide better illumination below the salt finger where streamer and OBN data cannot image clearly.

Conclusion

By placing most receivers below salt, VSP data has less wave propagation distortion and suffers less from complicated overburden effects. Therefore, VSP data can provide higher resolution and better illuminated images around the wellbore to complement existing towed-streamer and OBN data. However, VSP processing and imaging can be challenging and specialized workflows may be needed. The Atlantis 3D VSP case study highlights two unique VSP processing challenges that require special consideration and appropriate techniques to unlock the imaging potential of the survey. XYZ vector fidelity reorientation, using a crosscorrelation-based algorithm with rotation angle constraints and an anchor method for phase I data, was able to obtain reasonable reorientation angles, which resulted in better event coherency in the migrated images for X and Y components. Despite the efforts, there may be some uncertainty for the angles obtained due to data quality and an inaccurate salt model around the complicated salt finger area. Additionally, LSRTM had a great impact on the subsalt image by reducing the strong illumination patterns caused by the receivers being placed through the complicated salt finger, resulting in more coherent amplitude across receivers on the migrated receiver gathers. As a result, the illuminated area of the VSP image was largely expanded and the swing noise was also attenuated.

Acknowledgments

We thank BP, BHP, and CGG for permission to publish this work. We also thank Leon Zhu and Yan Huang for their significant contribution and fruitful discussions.

10.1190/segam2018-2996268.1

REFERENCES

Dy, S., W. Gou, C.-C. Lee, and W. Kim, 2016, Elastic modeling-based three-component VSP coordinate reorientation: 86th Annual International Meeting, SEG, Expanded Abstracts, 5628–5632, https://doi.org/10.1190/segam2016-13952514.1.

Roberts, M., T. Dy, S. Ji, M. Reasnor, and D. Shepherd, 2011, Improving Atlantis TTI model building. OBN+NATS, prism waves & 3D RTM angle gathers: 81th Annual International Meeting, SEG, Expanded Abstract, 3238–3242, https://doi.org/10.1190/1.3627868.

Shen, X., I. Ahmed, A. Brenders, J. Dellinger, J. Etgen, and S. Michell, 2017, Salt model building at Atlantis with full- waveform inversion: 87th Annual International Meeting, SEG, Expanded Abstracts, 1507–1511, https://doi.org/10.1190/segam2017-17738630.1.

Wang, P., A. Gomes, Z. Zhang, and M. Wang, 2016, Least-squares RTM: Reality and possibilities for subsalt imaging: 86th Annual International Meeting, SEG, Expanded Abstracts, 4204–4209, https://doi.org/10.1190/segam2016-13867926.1.